

Sensitivity studies have also been conducted for the parameters involved in the problem.⁵ These different choices of pursuer's constants show that the optimum values of $t_f - t_N$ for initial conditions in area A of Fig. 7 vary with the choice of missile parameters, and that the shape and size of all the areas of control philosophies are affected by these choices. Generally an increase in a or $G_{P_{\max}}$ or a decrease in τ_P reduces $r(t_f)$. The velocities, however, enter the picture in a much more interesting manner. It appears in fact that for a given V_E there is an optimum V_P . This will be reported on at a later date.

In closing, it should be noted that the research conducted considered only $0 \leq \phi(0) \leq 180^\circ$. However, the problem is symmetrical, and for $180^\circ \leq \phi \leq 360^\circ$ it is only necessary to use the negative of the control sequence. Figure 7 summarizes the results of the investigation. It is not claimed that the areas in this graph represent the actual size or shape of the true areas of target control philosophies. The initial conditions actually investigated for this graph include only the vicinity of the area enclosed by the intersection of line A and B, as may be seen by examining Fig. 2. The extensions are reasonable guesses.

References

- Ho, Y. C., Bryson, A. E., Jr., and Baron, S., "Differential Games and Optimal Pursuit-Evasion Strategies," *IEEE Transactions on Automatic Control*, Vol. AC-10, No. 4, Oct., 1965, pp. 385-389.
- Balakrishnan, A. V. and Neustadt, L. N., *Computing Methods in Optimization Problems*, Academic Press, New York, 1964, pp. 71-77.
- Bryson, A. E., Jr. and Ho, Y. C., *Applied Optimal Control*, Blaisdell, Waltham, Mass., 1969, pp. 287-288.
- Harvey, C. A., "Optimal Evasion (in Case Proportional Navigation is the Pursuit Strategy)," Appendix C, "The Calculus of Aerial Combat," R-RD 6418, May 1969, Honeywell Systems and Research Division, Minneapolis, Minn.
- Julich, P. M. and Borg, D. A., "Effects of Parameter Variations on the Capability of a Proportional Navigation Missile Against An Optimally Evading Target in the Horizontal Plane," LSU-T-TR-24 (thesis), 1969, Louisiana State Univ., Baton Rouge, La.

Pulse Heating and Equilibration of an Insulated Substructure

P. J. SCHNEIDER* AND C. F. WILSON JR.†
Lockheed Missiles and Space Company
Sunnyvale, Calif.

Nomenclature

- c = specific heat, Btu/lb-°F
 D = pulse heating duration, sec
 Fo_i' = modified Fourier number = $\alpha_i D / 2\pi \delta_i^2$, $i = 1, 2$
 k = thermal conductivity, Btu/sec-ft-°F
 n, n' = $\rho_2 c_2 \delta_2 / \rho_1 c_1 \delta_1$ and $\rho_2 k_2 / \rho_1 k_1$, respectively
 Q'' = total heat input = $q''_{\max} D / 2$, Btu/ft²
 q'' = instantaneous heat input, Btu/sec-ft²
 T = dimensionless temperature rise = $(k_1 / \delta q''_{\max} Fo_1') (t - t_0)$
 t = plate temperature, °F

- t_{eq} = equilibrium temperature = $t_0 + \pi \delta_1 q''_{\max} Fo_1' / (n + 1) k_1$, °F
 X = x / δ_1 ; x = depth from heated face, ft
 α = thermal diffusivity = $k / \rho c$, ft²/sec
 δ = thickness, ft
 Θ = $2\pi(\theta/D)$; θ = time, sec
 ρ = density, lb/ft³

Subscripts

- eq = equilibrium
max = maximum
0 = initial value ($\theta \leq 0$)
1, 2 = outer and inner layers, respectively

Introduction

A HEAT-CONDUCTION problem that recurs in aerospace systems design involves exposure of a two-layer plate to symmetrical pulse heating of the form

$$q'' = q''_{\max} \sin^2 \pi \theta / D \quad (1)$$

Usually the outer layer is of lower thermal conductivity than the inner load-bearing layer. As such, significant temperature gradients develop only in the outer insulation and the inner substructure can be taken to respond isothermally (Fig. 1). Examples include ascent-phase aerodynamic heating of rocket boosters and payloads, aerodynamic heating of re-entry vehicles, and flash heating of objects such as near exposure to nuclear detonations. These applications encompass such large excursions in environment, material properties, and individual layer thicknesses that it was deemed worthwhile to solve the two-parameter problem, including post-heating equilibration, in a general manner.

Analytical Model

The dimensionless differential equations and boundary conditions for the constant-property, two-layer plate system with no surface decomposition or surface reradiation, a high-conductivity inner layer ($k_2 \rightarrow \infty$), and an adiabatic rear face are:

$$\Theta \leq 0 \text{ (initial condition); } T_1 = T_2 = 0, \quad 0 \leq X \leq 1 \quad (2)$$

$$0 < \Theta \leq 2\pi \text{ (pulse heating);}$$

$$\partial T_1 / \partial X = -(1/Fo_1') \sin^2 \Theta / 2, \quad X = 0 \quad (3)$$

$$\partial^2 T_1 / \partial X^2 = (1/Fo_1') \partial T_1 / \partial \Theta, \quad 0 < X < 1 \quad (4)$$

$$T_1 = T_2, \quad X = 1 \quad (5)$$

$$\partial T_1 / \partial X = -(n/Fo_1') \partial T_2 / \partial \Theta, \quad X = 1 \quad (6)$$

$2\pi < \Theta \leq \Theta_{eq}$ (adiabatic equilibration); Eqs. (4-6) apply, and

$$\partial T_1 / \partial X = 0, \quad X = 0 \quad (7)$$

The three dimensionless variables are T , X , and Θ , and the two dimensionless parameters are Fo_1' and n . The more general case of finite k_2 introduces a third free parameter n' . Equations (2-7) refer to the special case of large k_2 where $n' \rightarrow \infty$. Low values of n correspond to thick insulation δ_1 or insulation with large ρc relative to the underlying substructure.

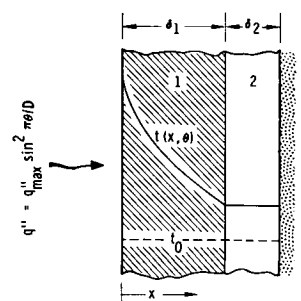


Fig. 1 Two-layer plate.

Presented as Paper 70-14 at the AIAA 8th Aerospace Sciences Meeting, New York, January 19-21, 1970; submitted February 11, 1970; revision received June 25, 1970.

* Staff Engineer, Missile Systems Division.

† Senior Thermodynamics Engineer, Aero-Thermodynamics, Missile Systems Division.

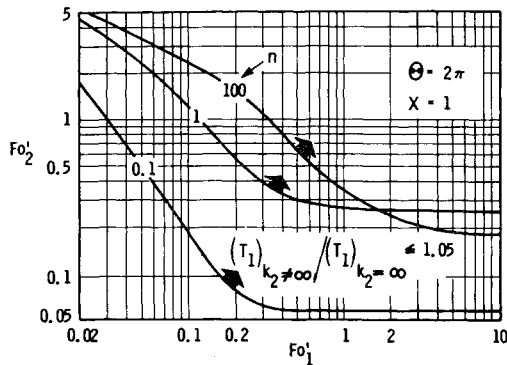


Fig. 2 Isothermal substructure criterion.

ture. Low values of Fo_1' correspond to good insulation (low k_1) and/or short heating duration D .

The general two-layer problem with both layers of finite conductivity, $n \neq 0$ and $n' \neq \infty$, was solved in 1959 for $0 < \Theta \leq 2\pi$, but only for the case of constant q'' .¹ The simpler case of constant q'' with $n \neq 0$ and $n' = \infty$ was treated in 1969 by exact methods.² The case $n = 0$ but with a pulse heat input was solved exactly in 1957 for $0 < \Theta \leq 2\pi$ only.³ The more general case $n \neq 0$ and $n' = \infty$ with a pulse heat source was treated by an approximate integral method in 1960, again for $0 < \Theta \leq 2\pi$ only.⁴ Thus, prior to the present work no accurate and complete solution existed for pulse heating with $n \neq 0$, $n' = \infty$, and $0 < \Theta \leq \Theta_{eq}$.

Solution Method

Equations (2-7) were solved for both the heating and adiabatic equilibration periods by an explicit finite-difference numerical scheme, using a high-speed digital computer to perform the calculations. A typical subdivision involved 30 nodes across the composite, this number ranging from 3 for large Fo_1' to 300 for small Fo_1' . Eight digits were carried in all calculations to minimize round-off errors (only minor cumulative errors were detected in approach to equilibrium). Conservatively small time steps were adopted to insure stable solutions without excessive run times. Typical runs required from 1-10 sec. The longest runs (400 sec) occurred when the response calculations were carried to equilibrium with combinations of high n and low Fo_1' . Detailed convergence studies performed as a function of node density suggest that in general both surface and substructure temperatures are accurate to within 1%. A general accuracy of 0.5% was confirmed for $n = 0$ by comparison with data from Ref. 5. Accuracy of 1% on maximum surface temperature at low Fo_1' was established by comparison with the semi-infinite solid case in Ref. 6.

One additional side study was undertaken prior to generating production solutions for the purpose of developing a quantitative criterion for judging when the isothermal substructure assumption breaks down due to finite n' . Point solutions for the general two-layer problem were generated for $0.01 \leq Fo_1' \leq 200$ and $0.1 \leq n \leq 100$ over a range of n' . Selected results are summarized in Fig. 2. The curves give the value of Fo_2' for which the interface temperature at the end of heating exceeds its corresponding value when $k_2 = \infty$ by 5%. If the actual Fo_2' in a given problem exceeds that given in Fig. 2 at the characteristic Fo_1' and n of that problem, then the substructure can be regarded as isothermal.

Response Data

Selected data for the insulated substructure system are given in Fig. 3 in terms of dimensionless temperature rises at the heated surface and interface for $n = 0.1, 1$ and 10 .†

† Additional data for $n = 0, 0.5, 5, 50$ and 100 are given in Ref. 7.

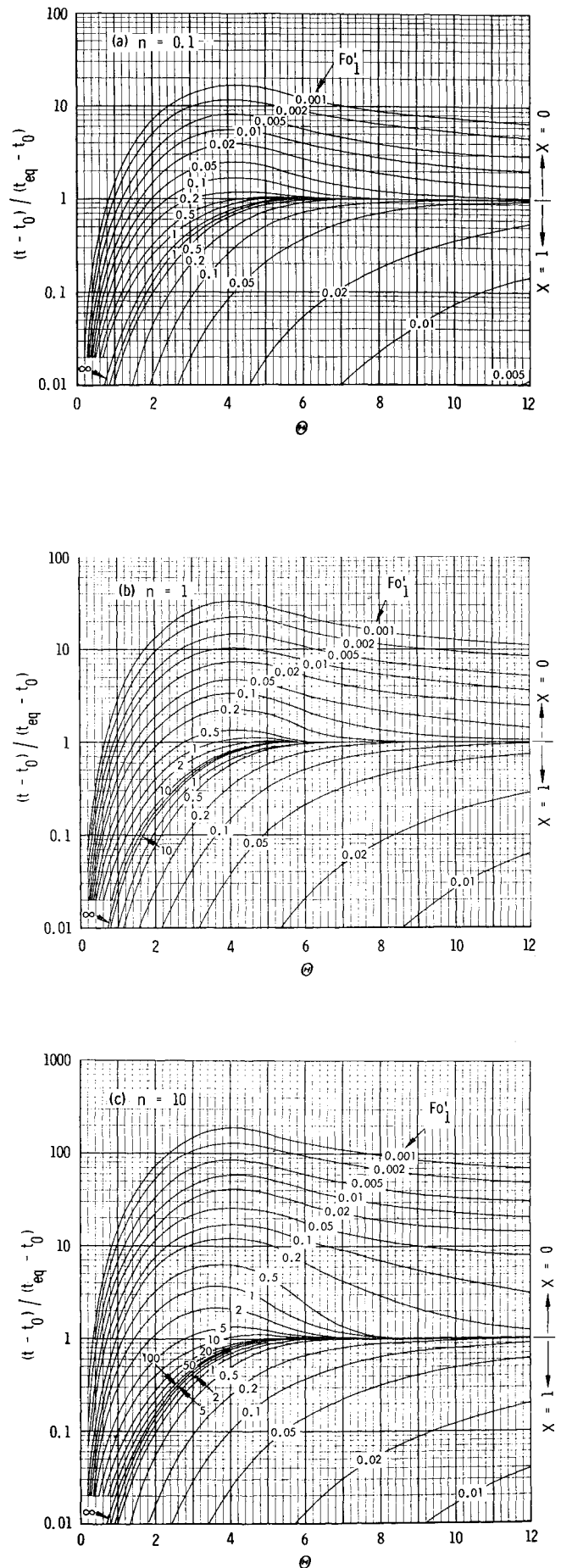


Fig. 3 Temperature response of heated surface and interface.

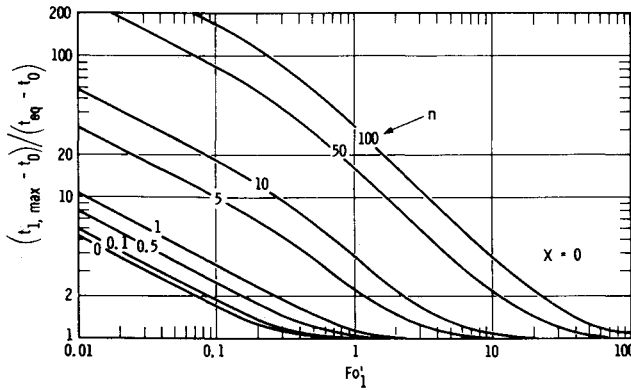


Fig. 4 Maximum temperature of heated surface.

These plate temperature rises are normalized by steady-state equilibrium values achieved after adiabatic equilibration

$$T_{eq} = \pi / (n + 1) \quad (8)$$

As $k_1 \rightarrow \infty$, $Fo_1' \rightarrow \infty$ and

$$T/T_{eq} = (\Theta - \sin\Theta) / 2\pi \quad (9)$$

This is the curve marked ∞ , common to all three charts; curves above this refer to the heated surface ($X = 0$), and those below are for the interface ($X = 1$) or substructure.

Figure 4 shows the normalized peak surface temperature $T_{1,max}$ with n as parameter. All curves have the same constant slope up to about $Fo_1' = 0.1$. For $Fo_1' < 0.1$, $T_{1,max}$ behaves as if the outer layer were semi-infinite, and in this region

$$T_{1,max}/T_{eq} \doteq (\frac{4}{3})(n + 1) / (2\pi Fo_1')^{1/2} \quad (10)$$

The exact behavior of $t_{1,max}$ is obscured because t_{eq} is in itself a function of both the independent variable Fo_1' and parameter n . In fact, at a given Fo_1' , $t_{1,max}$ decreases monotonically with increasing n .

Figure 5 gives dimensionless time Θ when $t_{1,max}$ occurs at $X = 0$. This time is independent of Fo_1' below about $Fo_1' = 0.1$ (see Fig. 3). The limit for low Fo_1' is verified by referring to the exact solution for surface temperature response of a semi-infinite solid ($x \geq 0$) exposed to pulse heating⁶:

$$[(\pi \rho c k / D^{1/2}) / q''_{max}] (t - t_0)_{x=0} = \frac{2}{15} \left(\frac{2}{\pi} \right)^{1/2} \Theta^{5/2} \left[1 - \frac{(2\Theta)^2}{7.9} + \frac{(2\Theta)^4}{7.9 \cdot 11 \cdot 13} - \dots \right] \quad (11)$$

This corresponds to $n = 0$ and $Fo_1' = 0$ ($\delta_1 \rightarrow \infty$). Maximum

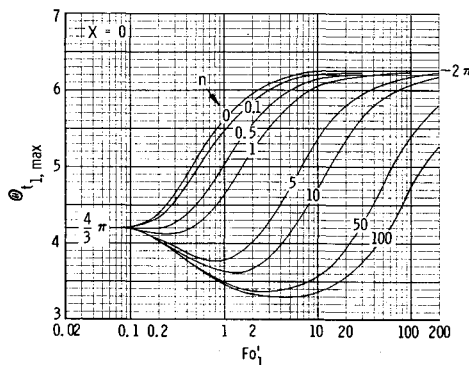


Fig. 5 Time of maximum heated-surface temperature.

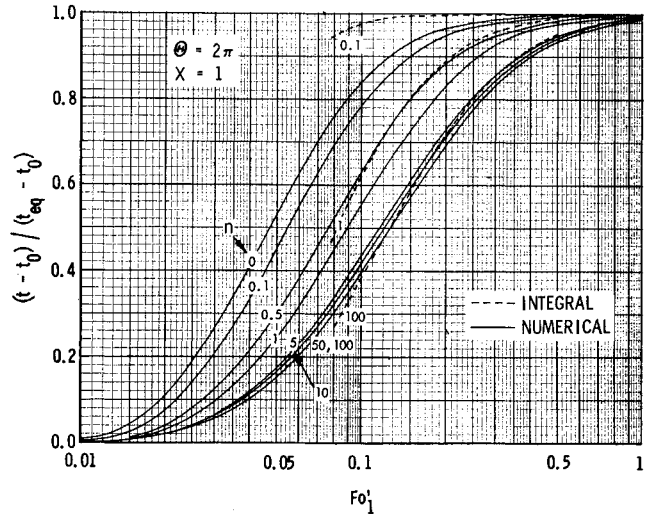


Fig. 6 Interface temperature at end of heating.

surface temperature occurs at $\Theta = (\frac{4}{3})\pi = 4.189$ or $\theta = (\frac{2}{3})D$. The asymptote for high Fo_1' ($\delta_1 \rightarrow 0$) is 2π or $\theta = D$. Thus, for $n = 0$ (single layer) the heated-surface temperature peaks $\frac{2}{3}$ through the heating pulse if the layer is thick, and at the end of the pulse if thin, the behavior being monotonic in between. For finite n , changing Fo_1' in Fig. 5 is thought of as varying k_1 . Increasing k_1 with large n has at first the effect of pushing the occurrence of peak surface temperature back toward the middle of the heating pulse $D/2$. This happens because with a massive substructure the interface temperature is held near t_0 , and the conductive flux from the heated surface more nearly follows the heat input q'' . As k_1 increases further, the outer layer once again behaves as if it were thermally thin with peak surface temperature being at $\theta = D$. A minimum occurs at intermediate Fo_1' for $n > 0.5$, its value approaching π for $n = 100$.

Figure 6 shows the important substructure response T_2 at the end of heating. The dashed curves for $n = 0.1, 1$, and 100 are from the approximate integral solution⁴

$$\frac{T}{T_{eq}} = \frac{(n + 1)}{2} \left\{ \frac{3}{2} (1 - X^2)(\Theta - \sin\Theta) + \frac{1}{Fo_1'} \left(\frac{3}{4} X^2 - X + \frac{1}{4} \right) (1 - \cos\Theta) - \pi \left[\left(\frac{3n + 1}{n + 1} \right) - 3X^2 \right] \frac{T_2(2\pi)}{T_{eq}} \right\} \quad (12)$$

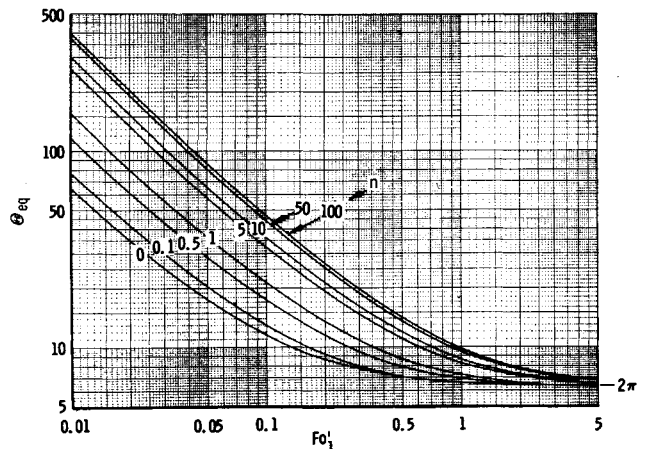


Fig. 7 Elapsed time from start of heating to end of adiabatic equilibration.

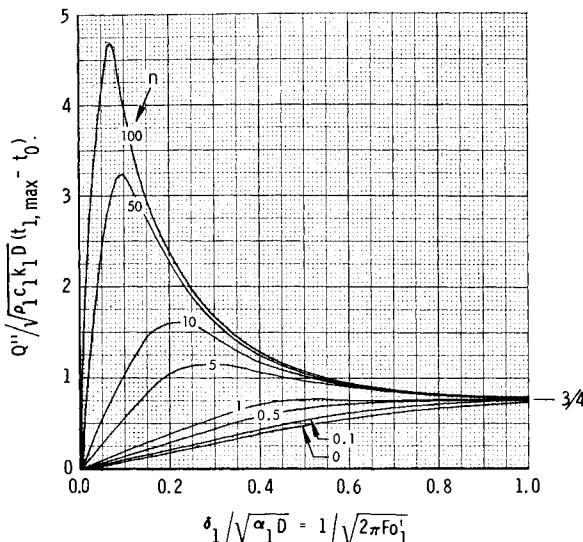


Fig. 8 Maximum heat absorption of single and two-layer plates.

where

$$\frac{T_2(2\pi)}{T_{eq}} = 1 - \frac{1}{12\pi F o_1'} \left(\frac{1/n - 3}{1/n - 1} \right) \times \left\{ \frac{1 - e^{-6\pi(1/n + 1)F o_1'}}{1 - [3(1/n + 1)F o_1']^2} \right\}, F o_1' \geq 0.0777$$

This integral solution is evidently a poor approximation for the rear-layer response, especially at low values of n .

The time required to reach thermal equilibrium Θ_{eq} , measured from the start of heating, is given in Fig. 7. Equilibration takes longer as the substructure becomes more massive and/or as the outer layer becomes more insulative.

Figure 8 gives a correlation of the heat-sink capability of an insulated substructure in terms of total heat absorbed $Q'' = q''_{max} D/2$ for a maximum permissible exposed-surface temperature rise $t_{l,max} - t_0$. For $n = 0$, increasing thickness increases the total permissible heat load Q'' that can be absorbed without exceeding $t_{l,max}$. This trend continues until the wall becomes thermally semi-infinite, at which point

$$Q'' = \left(\frac{3}{4}\right)(\rho_1 c_1 k_1 D)^{1/2}(t_{l,max} - t_0) \quad (13)$$

To trace the analogous trend for increasing δ_1 with finite n , it is necessary to imagine δ_2 increasing at the same rate as δ_1 (constant n). At low n and low δ_1 the effect is to first increase Q'' over that where no substructure exists. This increase becomes dramatic for large n , a peak in each curve occurring when δ_1 becomes large enough to overshadow the substructure, and the system becomes self-insulating. Thus, all curves approach the same asymptote ($\frac{3}{4}$) for semi-infinite insulation.

The over-all heat-sink performance of a two-layer plate can exceed that of an equal-weight, single-layer plate of either material. This is accomplished by using an outer layer with a high allowable temperature limit over a second material of lower allowable temperature but higher conductivity. Examples of composites that exhibit this characteristic are oxides over pure metals (e.g., beryllium oxide over beryllium) and pure metal composites such as molybdenum over copper.¹ Considering the latter example with $t_0 = 70^\circ\text{F}$ and $D = 15$ sec, a single copper plate gives $q''_{max} = 1250$ Btu/sec-ft², and a single molybdenum plate 1630 Btu/sec-ft² if melting is not allowed. The combination of molybdenum over $\frac{1}{2}$ " copper gives $q''_{max} = 1760$ Btu/sec-ft², an improvement of 8% at a penalty of 25% increase in section weight (lb/ft²) over molybdenum alone.

References

- ¹ Halle, H. and Taylor, D. E., "Transient Heating of Two-Element Slabs Exposed to a Plane Heat Source," CML-59-M-1, May 1959, Chicago Midway Labs., Chicago, Ill.
- ² Mikhaylov, M. D., "Transient Temperature Fields in Shells," TT F-552, June 1969, NASA.
- ³ Wilson, L. H., Tucker, M., and Brandt, W. E., "Atmospheric and Hypersonic Phenomena: Entry Problem—Preliminary Heat Sink Design Studies of the Polaris Re-Entry Body," *Proceedings of the 4th U. S. Navy Symposium on Aeroballistics, Bureau of Ordnance, NAVORD 5904*, 1957.
- ⁴ Thomas, P. D., "Approximate Analytical Solutions to Transient Heat Conduction in Finite Slabs With Arbitrary Heat Input," TIAD 148, April 1960, Lockheed Missiles & Space Company, Sunnyvale, Calif.
- ⁵ Schneider, P. J., *Temperature Response Charts*, Wiley, New York, 1963.
- ⁶ Thomas, P. D., "Prediction of Time at Which Surface Melting Begins for a Solid Subjected to Transient Heating," DD 16243, Oct. 1959, Lockheed Missiles & Space Company, Sunnyvale, Calif.
- ⁷ Schneider, P. J. and Wilson, C. F., Jr., "Pulse Heating and Equilibration of an Insulated Substructure," AIAA Paper 70-14, New York, 1970.

Computer Solution to Generalized One-Dimensional Flow

E. WILLIAM BEANS*

Ohio State University, Columbus, Ohio

Introduction

ANY text on gas dynamics describes the simple flow processes which involve only area change, total temperature change, or friction, and a number of methods for solving problems involving all three effects have been presented in the literature; namely, 1) the use of Crocco functions,¹ 2) the use of polytropic exponents,² and 3) the use of constant dependent parameters.³ However, both the Crocco function $pA^{(\epsilon-1)/\epsilon} = \text{constant}$ and the polytropic exponent $(p/\rho^n = \text{constant})$ require that ϵ or n be known from experimental data. Here p , A , and ρ are the pressure, area, and density, respectively. Also, the value of ϵ or n is not singularly related to the independent parameters which control the flow, such as total temperature T_0 and area ratio. For example, by varying the pressure ratio across the duct, the Mach number M and pressure distributions will change, even though T_0 and area ratio are unchanged. Hence, the value of ϵ or n will change independent of T_0 and A . The third, use of constant dependent functions, has limitations in that it can only solve problems in which such parameters as temperature or pressure are held constant. Many of these processes are of little practical interest. Also, the use of constant dependent functions specifies the relationship between A , T_0 , and friction; hence, generality is lost.

It is possible using electronic computers to apply the method of influence coefficients⁴ to one-dimensional flow problems involving simultaneous variations in A , T_0 , and friction. The method described here is for the case of fluids having constant composition and a constant ratio of specific heats k . These assumptions are made only for the sake of brevity. The method of influence coefficients as used in fluid mechanics is a set of differential equations obtained from combining the momentum, continuity and energy equations, and equations of state. The only limitations to the method are the assumption

Received June 18, 1970; revision received August 13, 1970.

* Assistant Professor. Member AIAA.